

# Supporting Information

Edwards et al. 10.1073/pnas.1710480115

## SI Materials and Methods

**Cell Culture and Transformation and Inductions.** For all experiments, *D. discoideum* AX2 strains were grown in HL5 medium on tissue culture-treated plastic 100 mm (Greiner CELLSTAR) or 150 mm (Falcon) plates to 70 to 90% confluency at 22 °C (1). Fluorescent imaging was performed in developmental buffer (DB) [phosphate buffer (PB) supplemented with 2 mM MgSO<sub>4</sub> and 0.2 mM CaCl<sub>2</sub>]. For plasmid transformation and exogenous gene expression, cells were transformed using electroporation as previously described (2). Cells carrying expression constructs were placed under antibiotic selection using either 20 to 30 μg/mL G418 or 50 μg/mL Hygromycin B. For experiments imaging fluorescence or developed cells undergoing chemotaxis, the cells were gently washed and then resuspended in DB and placed onto four-chamber glass slides (Nunc Lab-Tek) with 200 μL of DB.

**Expression Constructs and Knockout Strains.** The *pten*<sup>-</sup> strain was created in our laboratory and described previously (3). *pkbA*<sup>-</sup> and *pkbR1*<sup>-</sup> strains were described previously (4, 5). Rap1 and RasC plasmids were described previously (5). LimE<sub>Δcoil</sub>-RFP, PH<sub>Crac</sub>, and RBD plasmids were obtained from dictyBase (6) previous studies. RAM<sup>-</sup> mutants were previously described (7). R1-Akt expression construct was created in our laboratory and described previously (4). Rap1 and RasC constructs were induced with 10 g/mL doxycycline (Sigma) in vector pdm359 (8).

**Immunoblotting.** To examine protein levels and posttranslational modifications, 1 × 10<sup>6</sup> cells per 10 μL of 1× lysis buffer was collected by centrifugation and loaded into 4 to 20% Tris-HCl polyacrylamide gel (Bio-Rad Criterion). Protein concentrations were determined by Bradford protein assay for normalizing loading. Protein was transferred to Immobilon-FL PVDF Membrane (Millipore), and immunoblotted as previously described (9). Primary antibodies were incubated overnight, and fluorescent-conjugated secondary antibodies were as prepared and used as per manufacturer (LI-COR Biosciences) instructions. Blots were imaged on a LI-COR Odyssey CLx at high resolution, and signal intensities were measured in the associated software. The primary antibodies used in these studies were all obtained from Cell Signaling: Anti-Phospho-Akt (PKC $\zeta$ ) substrate 1:2,000 (RXXS\*/T\*, 110B7E[40]), Anti-Actin C4 1:10,000 (MAB1501), Anti-Phospho PKC (pan) antibody (190D10 Rabbit Monoclonal, catalog no. 2060), and Anti-Phospho-Akt (S473) (catalog no. 9271), all at 1:1,000 dilution.

**Cell Survival and Replating Assay.** To assay cell survival, we quantified colony forming units via a replating assay on SM agar plates (10). For survival assays, cells were plated at a density of 4 × 10<sup>4</sup> cells per square centimeter on four-chambered slides (Nunc Lab-Tek). Cells were washed off into a solution containing 200 μL of an overnight culture of *Klebsiella aerogenes* and resuspended in DB buffer. A 200-μL aliquot of the resulting *Dictyostelium/Klebsiella* solution was then spread evenly on SM agar plates. Plates were incubated at 22 °C for 36 h, and then the number of discrete colonies on each plate was determined. Percentage survival was determined from the ratio of the number of colony forming units at each time point to the number of colony forming units at time 0. Assays were performed in triplicate for each time point.

**Microscopy and Image Processing.** Time-lapse phase-contrast imaging was performed on a Zeiss Observer Z.1 microscope and a Zeiss Axiovert 200M microscope (Axiovision software) using 10× 0.45 N.A. or 40× 0.95 N.A. objectives. All images were processed using NIH ImageJ. Confocal imaging was performed on a Zeiss LSM780 single-point laser-scanning microscope (Zeiss AxioObserver with 780-Quasar confocal module; 34-channel spectral, high-sensitivity gallium arsenide phosphide detectors) with a 63×/1.5 N.A. objective. Total internal reflection fluorescence (TIRF) microscopy was carried out with a Nikon Eclipse TiE microscope illuminated by an Ar laser (YFP) and diode laser (mCherry) with a 100×/1.5 N.A. objective. Images were acquired by a Photometrics Evolve EMCCD camera controlled by Nikon NIS-Elements software. Structured illumination microscopy (SIM) was performed on a Nikon N-SIM microscope controlled using a 100× 1.4 N.A. objective and an Andor EMCCD camera controlled by NIS-Elements. Kymographs were generated using a custom MATLAB (MathWorks) script described previously (11). Colors were assigned in a linear fashion for all kymographs, with blue indicating the lowest intensity, and red the highest.

**Quantifying Cytoskeletal Puncta and t-Stacks.** F-actin puncta under confocal microscopy were defined patches of activity whose intensity was 2 SD above the mean cytosolic intensity (12). The start and end of puncta were defined by a 2 SD ± 10% benchmark. Inhibitor experiments were performed with 50 μM LY294002 (catalog no. 9901; Cell Signaling) or with 40 μM PP242 (catalog no. 4257; Tocris) in 0.1% DMSO for 1 h. Background was subtracted from all puncta intensity measurements. ImageJ (NIH) software was used for processing and analysis of t-stacks as previously described (12). Confocal time-lapse videos were first converted to grayscale in ImageJ and then background subtracted and sharpened. The ImageJ 3D Viewer plugin was then used to stack the frames from the video. The resampling factor was set to 1 to avoid blurring between frames.

**Global Stimulation.** Global stimulation experiments were performed by adding folate to a final concentration of 1 mM to cells on a four-chambered glass slide (9). Images were acquired at 1-s intervals. The change in cytosolic intensity of F-actin marker LimE<sub>Δcoil</sub>-RFP was measured using imageJ as a proxy for the relocalization of F-actin to the membrane upon stimulation. To quantify relative changes, we divided the cytosolic intensity by the intensity at time 0 for each strain. We analyzed at least 10 cells and plotted the average at each time point. Pancake cells were generated by induction with doxycycline for 10 h before experiment.

**Flatness Measures.** To quantify the change in cell spreading, we computed a flatness parameter, F, using the ratio of the square root of the basal surface area (a) to the cube root of the volume (v):  $F = a^{1/2}/v^{1/3}$  (7, 13). F is independent of the object's volume and can be compared across different cell types. Flatness was computed from isosurface renderings of confocal z-stacks by using the Imaris (Bitplane) measurement tool to obtain volume and basal surface area parameters. There were only slight differences in the volumes of pancake and parent cells. Changes in F values were due primarily to changes to the basal surface area/footprint of the cell caused by cell spreading. Blind observers routinely assigned cells with a flatness of >2 as a distinct population, which we defined as pancake cells.

**Phagocytosis and Pinocytosis.** For measuring pinocytosis, we used a modified version of a previously published pinocytosis assay (14, 15). Samples (10 mL) of  $5 \times 10^6$  cells per milliliter were shaken in 25-mL Erlenmeyer flasks at 120 rpm. TRITC-dextran  $60 \times 10^3$  (Sigma) was added to a final density of 2.5 mg/mL. Samples of 1 mL were withdrawn at desired intervals and added to 100  $\mu$ L of trypan blue solution to quench extracellular fluorescence. Samples were then centrifuged for 3 min at  $800 \times g$ . The cell pellet was washed once in 1 mL of PB (17 mM NaK-PB, pH 6.0) and resuspended in 1 mL of PB, and then relative fluorescence intensity was immediately measured in a Hitachi F-7000 fluorescence spectrometer at 545 nm for excitation and at 574 nm for emission. We used Western blots of cell samples to control for differences in volume and cell size between different strains used. For phagocytosis, TRITC-labeled *Saccharomyces* was made as described in Rivero and Maniak (15), and a modified version of the assay was used for the experiment. Briefly,  $1 \times 10^5$  cells in PB were added to a four-chambered glass plate and allowed to adhere for 30 min. Next,  $3 \times 10^5$  cells of TRITC-labeled yeast were added. After 30 min, chambers were washed three times with PB, and then 100  $\mu$ L of trypan blue solution was added to quench extracellular fluorescence. The number of cells taking up at least one yeast particle was then manually quantitated for 10 fields.

**Hypotonic Shock.** Cells were cultured in HL5 ( $\sim 130$  mOsmol) growth medium to a density of  $1 \times 10^6$ /mL then shifted to a

hyperosmotic condition consisting of NaCl-supplemented PB (240 mOsmol). After 10 min, cells were shifted to PB ( $\sim 25$  mOsmol) for 2 h. Replating assays were then performed as described above to determine viability.

**Cell Growth and Sparagmosis Assays.** Cell growth assays were conducted in HL5 media in suspension with doxycycline added at time 0 (1). Samples were taken at the indicated times for cell counting using a hemocytometer. Assays were conducted in triplicate. For sparagmosis assays in Fig. S7, cells were first induced in shaking culture with doxycycline. After 10 h, an aliquot ( $\sim 1 \times 10^5$  cells) was removed and added to a four-chambered glass slide. Replating assays were performed as described previously to determine percentage survival. Acrylamide surfaces (100 kPa and 0.1 kPa CytoSoft plates) were purchased from Advanced Bio Matrix. Chamber slides were treated with 1% (wt/vol) solutions of BSA for 4 h for the relevant experiments.

**Statistical Analysis.** When the values for different samples were matched within the experiment, either a paired two-tailed *t* test (for two samples) or repeated-measures ANOVA with a Student–Newman–Keuls posttest (for multiple samples) was used. When the number of samples varied between the groups, an unpaired two-tailed *t* test was used. A *P* value of  $<0.05$  was considered significant.

1. Sussman M (1987) Cultivation and synchronous morphogenesis of *Dictyostelium* under controlled experimental conditions. *Methods Cell Biol* 28:9–29.
2. Gaudet P, Fey P, Chisholm R (2008) Transformation of *Dictyostelium* with plasmid DNA by electroporation. *CSH Protoc* 3:pdb.prot5103.
3. Iijima M, Devreotes P (2002) Tumor suppressor PTEN mediates sensing of chemoattractant gradients. *Cell* 109:599–610.
4. Kamimura Y, et al. (2008) PIP3-independent activation of TorC2 and PKB at the cell's leading edge mediates chemotaxis. *Curr Biol* 18:1034–1043.
5. Cai Y, et al. (2010) Cytoskeletal coherence requires myosin-IIA contractility. *J Cell Sci* 123:413–423.
6. Fey P, Dodson RJ, Basu S, Chisholm RL (2013) One stop shop for everything Dictyostelium: dictyBase and the Dicty Stock Center in 2012. *Methods Mol Biol* 983:59–92.
7. Lampert TJ, et al. (2017) Shear force-based genetic screen reveals negative regulators of cell adhesion and protrusive activity. *Proc Natl Acad Sci USA* 114:E7727–E7736.
8. Veltman DM, Keizer-Gunnink I, Haastert PJ (2009) An extrachromosomal, inducible expression system for *Dictyostelium discoideum*. *Plasmid* 61:119–125.
9. Artemenko Y, Swaney KF, Devreotes PN (2011) Assessment of development and chemotaxis in *Dictyostelium discoideum* mutants. *Methods Mol Biol* 769:287–309.
10. Loomis WF (2015) Genetic control of morphogenesis in *Dictyostelium*. *Dev Biol* 402:146–161.
11. Miao Y, et al. (2017) Altering the threshold of an excitable signal transduction network changes cell migratory modes. *Nat Cell Biol* 19:329–340.
12. Huang CH, Tang M, Shi C, Iglesias PA, Devreotes PN (2013) An excitable signal integrator couples to an idling cytoskeletal oscillator to drive cell migration. *Nat Cell Biol* 15:1307–1316.
13. Vogel S (2013) *Comparative Biomechanics: Life's Physical World* (Princeton Univ Press, Princeton).
14. Maniak M, Rauchenberger R, Albrecht R, Murphy J, Gerisch G (1995) Coronin involved in phagocytosis: Dynamics of particle-induced relocalization visualized by a green fluorescent protein tag. *Cell* 83:915–924.
15. Rivero F, Maniak M (2006) Quantitative and microscopic methods for studying the endocytic pathway. *Methods Mol Biol* 346:423–438.







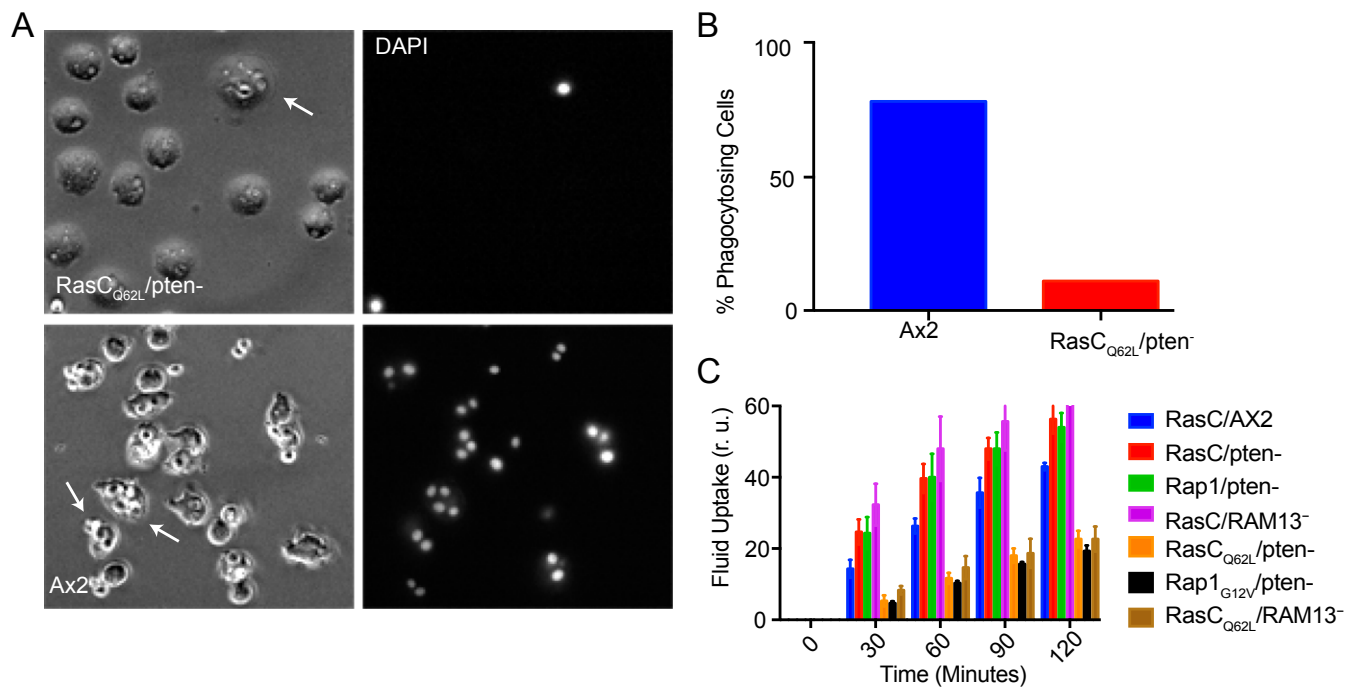


**Fig. 57.** Phagocytosis and pinocytosis are defective in pancake cells. (A) Representative images from phagocytosis assays with rhodamine-labeled yeast. Pancake cells (*Top*) very rarely phagocytose particles, unlike wild-type cells (*Bottom*). (Magnification: 40 $\times$ .) (B) Quantification of data in A.  $n = 150$  cells. (C) Pinocytosis of fluorescent dextran was analyzed in a plate reader for the indicated strains. RAM13 $^{-}$  and  $pten^{-}$  pancake cells (Rap1 $_{G12V}$  or RasC $_{Q62L}$  expressing) show an approximate threefold decrease in fluid uptake.

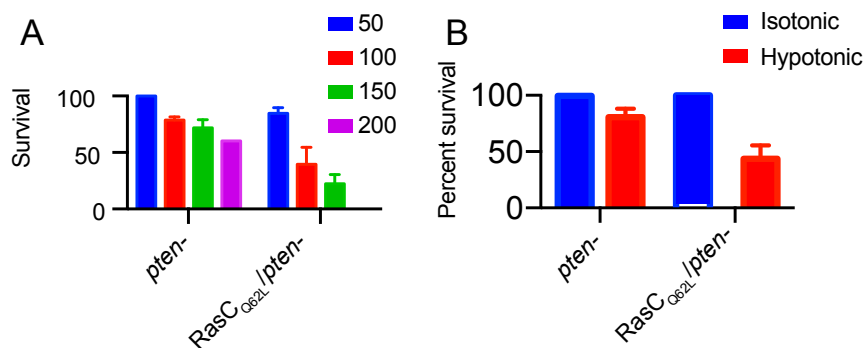


**Fig. 58.** Fragility of RasC $_{Q62L}/pten^{-}$  cells. (A) Replating assay documenting increased sensitivity to mechanical perturbation. Cells were shaken at 50, 100, 150, or 200 rpm for 30 min and then replated to determine viability (see *SI Materials and Methods*). RasC $_{Q62L}/pten^{-}$  pancake cells show a marked decrease in survivability at higher rpm. (B) RasC $_{Q62L}/pten^{-}$  cells are more sensitive to osmotic shock than their  $pten^{-}$  parental cells.  $n = 100$  cells for both assays.



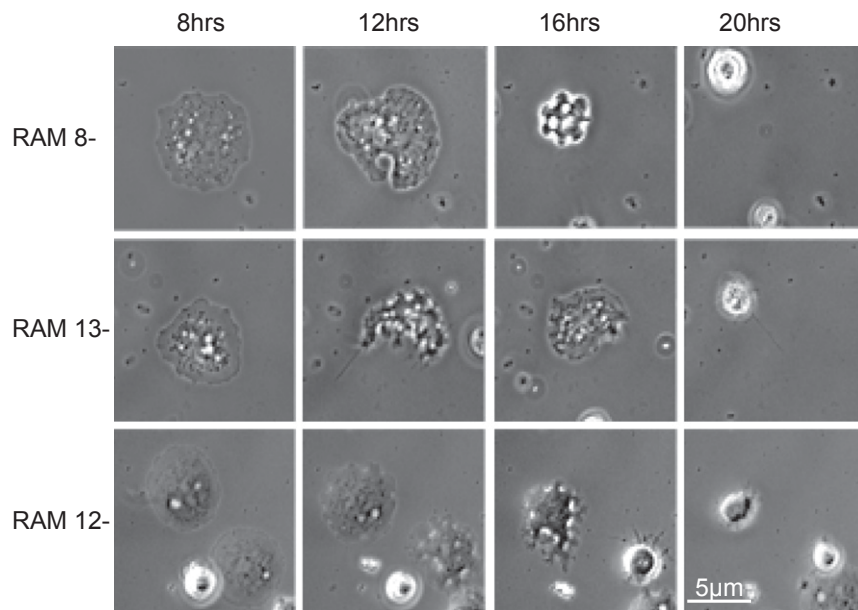


**Fig. S9.** Sparagmosis in  $RAM^{-}$  mutants. RAMs  $8^{-}$ ,  $11^{-}$ , and  $13^{-}$  transformed with the inducible  $RasC_{Q62L}$  construct were induced for 8 h with doxycycline and then imaged for 24 h. As with  $RasC_{Q62L}/pten^{-}$  cells,  $RAM^{-}$  cells expressing constitutively activated RasC sparagmosis at around the 10-h mark die by catastrophic fragmentation. Representative images at the indicated time points are shown. Images are at 40 $\times$  magnification.

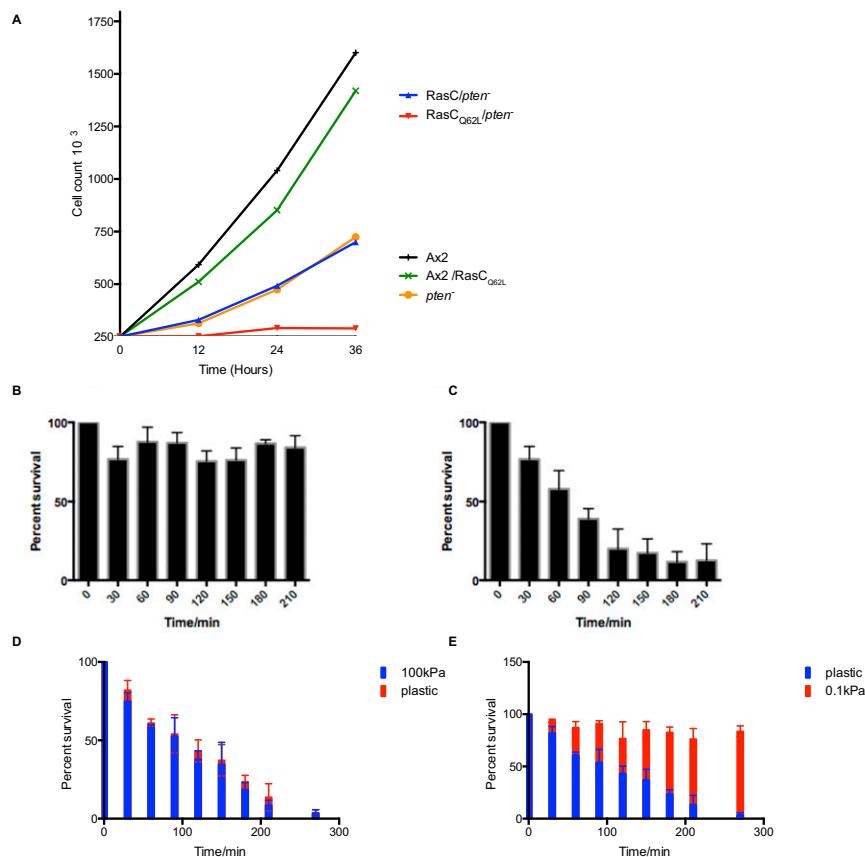


**Fig. S10.**  $RasC_{Q62L}$ -induced sparagmosis and cell death are impaired on soft substrates. (A) Cell counts of cultures grown in suspension cultures at 150 rpm. Aliquots were taken from cultures at the indicated time points for counting. Cells with induced  $RasC_{Q62L}$  have moderate to severe growth defects; however, there is little cell death determined by inspection under the microscope, and cell numbers remain constant for 36 h.  $RasC/pten^{-}$  (B) or  $RasC_{Q62L}/pten^{-}$  (C) was induced for 8 h in suspension, plated in Nunc-tek glass chambers, and then imaged for the 4 h. Cell survival was calculated by manually counting cell death events over an average of three  $10\times$  fields (200–300 cells total). (D) Cell death in  $RasC_{Q62L}/pten^{-}$  cells induced in suspension and then plated on plastic dishes or 100-kPa acrylamide pads in (B). (E) Cell death assays as in (B) and (D) on 0.1-kPa acrylamide pads.

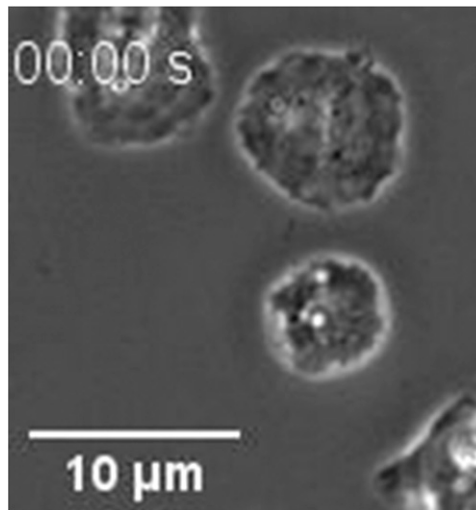
**Table S1. Phenotypic analysis of pairwise perturbations performed in this study**

Genotype	Other name	Morphology	Modifier	Rescue	Modified morphology
AX2 (RK/ME) WT		Wild-type	(Dox) RasC WT	NA	No change
AX2 (RK/ME) WT		Wild-type	(Dox) RasC Q62L	NA	Spread, fans, oscillators
AX2 (RK/ME) WT		Wild-type	(OE) Gbpd	NA	Spread, multinucleated
AX2 (RK/ME) WT		Wild-type	(Dox) RasC Q62L	(OE) Rap1 N17	Wild-type
AX2 (RK/ME) WT		Wild-type	(OE) Rap1 N17	NA	No change
AX2 (RK/ME) WT		Wild-type	(Dox) Rap1 wt	NA	No change
AX2 (RK/ME) WT		Wild-type	(Dox) Rap1 G12V	NA	Spread, fans, oscillators
PTEN $\Delta$		Flat, multiple pseudopods	(Dox) RasC WT	NA	No change
PTEN $\Delta$ *		Flat, multiple pseudopods	(Dox) RasC Q62L	NA	Pancake
PTEN $\Delta$		Flat, multiple pseudopods	(Dox) RasC Q62L	LY294002	Flat, multiple pseudopods
PTEN $\Delta$		Flat, multiple pseudopods	(Dox) Rap1 G12V	LY294002	Flat, multiple pseudopods
PTEN $\Delta$		Flat, multiple pseudopods	(Dox) RasC Q62L	PP242	Flat, multiple pseudopods
PTEN $\Delta$		Flat, multiple pseudopods	(Dox) Rap1 G12V	PP242	Flat, multiple pseudopods
PTEN $\Delta$		Flat, multiple pseudopods	(OE) Gbpd	NA	Giant, multinucleated cells
PTEN $\Delta$		Flat, multiple pseudopods	(OE) Rap1 N17	NA	Flat, multiple pseudopods
PTEN $\Delta$		Flat, multiple pseudopods	(Dox) Rap1 wt	NA	No change
PTEN $\Delta$ *		Flat, multiple pseudopods	(Dox) Rap1 G12V	NA	Pancake
PTEN $\Delta$		Flat, multiple pseudopods	(Dox) RasC Q62L	(OE) Rap1N17	ptenlike
PTEN $\Delta$		Flat, multiple pseudopods	(Dox) RasC Q62L	GFP-Pten	Flat
PTEN $\Delta$ *		Flat, multiple pseudopods	(Dox) RasC Q62L	GFP-PtenC1245*	Pancake
Actinbindin C $\Delta$	RAM1	Flat	(Dox) RasC WT	NA	Flat
Actinbindin C $\Delta$ *	RAM1	Flat	(Dox) RasC Q62L	NA	Pancake
Inversin $\Delta$ *	RAM4	Flat	(Dox) Rap1 G12V	NA	Pancake
Inversin $\Delta$	RAM4	Flat	(OE) Rap1 N17	NA	Flat
Inversin $\Delta$	RAM4	Flat	(Dox) RasC WT	NA	Flat
Inversin $\Delta$ *	RAM4	Flat	(Dox) RasC Q62L	NA	Pancake
SepA/STE kinase $\Delta$	RAM5	Flat, multinucleated	(Dox) RasC WT	NA	Flat
SepA/STE kinase $\Delta$	RAM5	Flat, multinucleated	(Dox) RasC Q62L	NA	Pancake
H-5-6-0 Sulfo. trans. $\Delta$	RAM6	Flat	(Dox) RasC WT	NA	Flat
H-5-6-0 Sulfo. trans. $\Delta$	RAM6	Flat	(Dox) RasC Q62L	NA	Pancake
Tenascinlike $\Delta$	RAM12	Flat	(Dox) RasC WT	NA	Flat
Tenascinlike $\Delta$ *	RAM12	Flat	(Dox) Rap1 G12V	NA	Pancake
Tenascinlike $\Delta$	RAM12	Flat	(Dox) RasC Q62L	LY294002	Flat
Tenascinlike $\Delta$	RAM12	Flat	(OE) Rap1 N17	NA	Flat
Tenascinlike $\Delta$	RAM12	Flat	(Dox) RasC Q62L	(OE) Rap1N17	Flat
Tenascinlike $\Delta$ *	RAM12	Flat	(Dox) RasC Q62L	NA	Pancake
DUSP19 $\Delta$	RAM13 <sup>-</sup>	Flat	(Dox) RasC WT	NA	Flat
DUSP19 $\Delta$ *	RAM13 <sup>-</sup>	Flat	(Dox) RasC Q62L	NA	Pancake
DUSP19 $\Delta$	RAM13 <sup>-</sup>	Flat	(Dox) RasC Q62L	GFP-Dusp19	Flat
DUSP19 $\Delta$	RAM13 <sup>-</sup>	Flat	(Dox) Rap1 wt	NA	Flat
DUSP19 $\Delta$	RAM13 <sup>-</sup>	Flat	(Dox) RasC Q62L	LY294002	Flat
DUSP19 $\Delta$ *	RAM13 <sup>-</sup>	Flat	(Dox) Rap1 G12V	NA	Pancake
DUSP19 $\Delta$	RAM12	Flat	(Dox) RasC Q62L	(OE) Rap1N17	Flat
DUSP19 $\Delta$	RAM13 <sup>-</sup>	Flat	(Dox) RasC Q62L	(OE) Rap1N17	Flat
DDB_G0270890 $\Delta$	RAM14	Flat	(Dox) RasC WT	NA	Flat
DDB_G0270890 $\Delta$	RAM14	Flat	(Dox) RasC Q62L	NA	Pancake
MyoII $\Delta$		Flat, multinucleated	(Dox) RasC WT	NA	Flat, multinucleated
MyoII $\Delta$		Flat, multinucleated	(Dox) RasC Q62L	NA	Flat, multinucleated

The table lists the base strain used and its phenotype, along with the modified phenotype produced by expressing a modifier gene or an additional "rescue" modifier gene intended to suppress or block the effect of the modifier. NA, not performed/attempted; OE, overexpressed;  $\Delta$ , gene knockout.

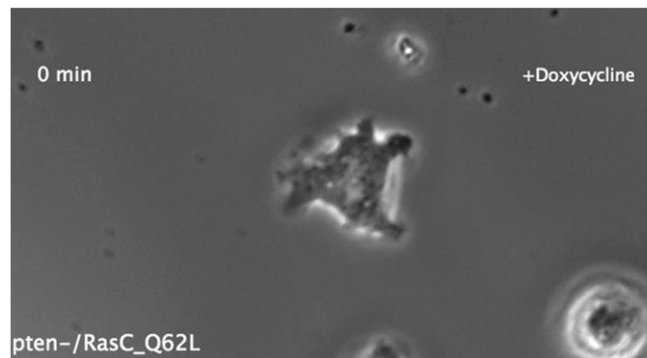
\*Experiments producing pancake cells that die by fragmentation.





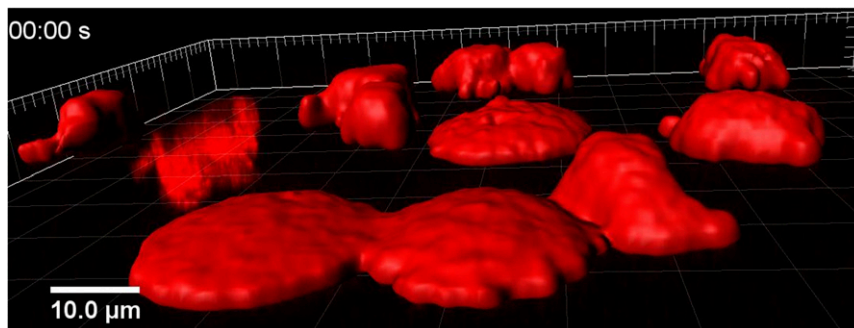
**Movie S1.** RasC oscillator. Induction of RasC<sub>Q62L</sub> expression in AX2 wild-type cells leads to an oscillatory phenotype. Cells rhythmically contract and spread in alternating cycles. Phase-contrast microscopy. (Magnification: 40 $\times$ .)

[Movie S1](#)



**Movie S2.** Pancake induction. Induction of RasC<sub>Q62L</sub> expression in *pten*<sup>-</sup> cells leads to massive cell spreading and flattening over the course of 8 h. Cells transition from the multiple-protrusion *pten*<sup>-</sup> phenotype to the flattened pancake phenotype. Phase-contrast microscopy. (Magnification: 40 $\times$ .)

[Movie S2](#)



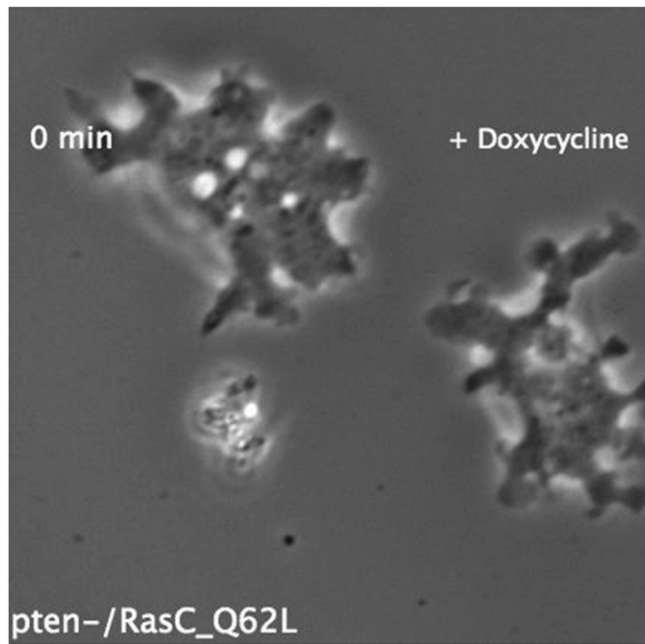
**Movie S3.** Isosurface renderings of pancake and *pten*<sup>-</sup> cells. Isosurface renderings of a mixed field of pancake and parental *pten*<sup>-</sup> cells. RasC<sub>Q62L</sub> and RasC (these cells retain a parental phenotype; Fig. 1) *pten*<sup>-</sup> cells were mixed before the induction of RasC expression by doxycycline. Z-section confocal movies were acquired after 8 h of induction. Renderings were done in Imaris. (Magnification: 63 $\times$ .)

[Movie S3](#)



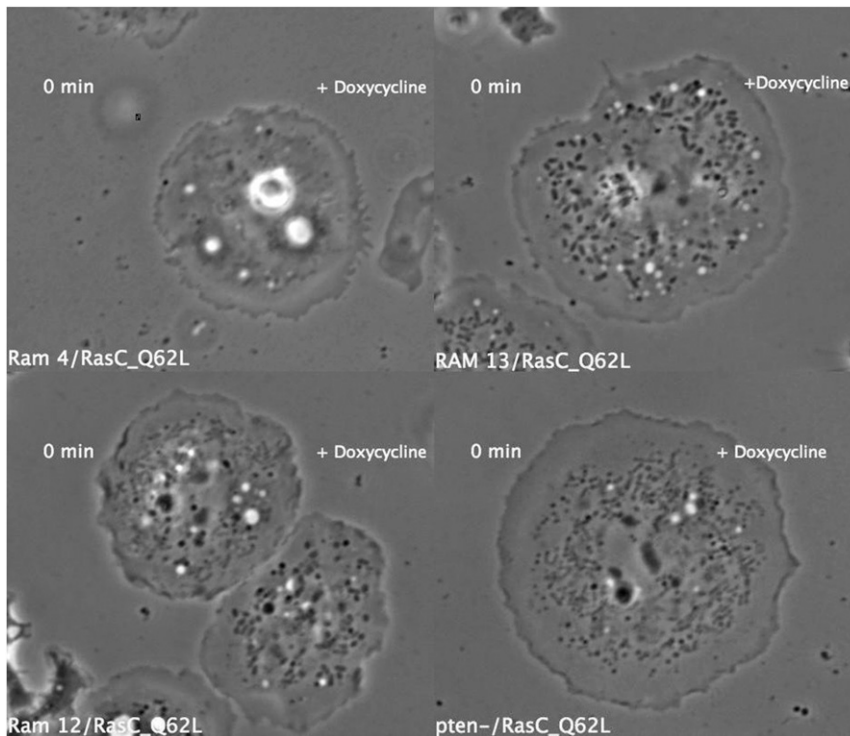






**Movie S10.** Sparagmosis in pancake cells.  $RasC_{Q62L}/pten^{-}$  cells undergo cell death by catastrophic cytoplasmic fragmentation within 48 h of induction of  $RasC_{Q62L}$  expression. Time-lapse was acquired 12 h after Ras induction by doxycycline. Phase-contrast microscopy. (Magnification: 40x.)

[Movie S10](#)



**Movie S11.** Sparagmosis in  $RAM^{-}$  pancake cells. Induction of  $RasC_{Q62L}$  expression in  $RAMs\ 4^{-}$ ,  $12^{-}$ ,  $13^{-}$ , and  $pten^{-}$  leads to catastrophic cytoplasmic fragmentation within 48 h of induction. Time-lapse was acquired 12 h after Ras induction by doxycycline. Phase-contrast microscopy. (Magnification: 40x.)

[Movie S11](#)